

Neutral-current reactions of solar and supernova neutrinos on deuterium

J. N. Bahcall

Institute for Advanced Study, Princeton, New Jersey 08540

K. Kubodera*

Department of Physics, State University of New York, Stony Brook, New York 11794

S. Nozawa

Swiss Institute for Nuclear Research, CH-5234, Villigen, Switzerland

(Received 29 December 1987)

We calculate the cross sections for the neutral-current disintegration of deuterium by neutrinos and antineutrinos: $\nu + d \rightarrow \nu' + n + p$ and $\bar{\nu} + d \rightarrow \bar{\nu}' + n + p$. We put special emphasis on estimates of the theoretical uncertainties of these cross sections. For ${}^8\text{B}$ and hep solar neutrinos, the averaged cross sections are $\langle\sigma({}^8\text{B})\rangle = 4.1(1\pm 0.1)\times 10^{-43}\text{ cm}^2$ and $\langle\sigma(\text{hep})\rangle = 1.15(1\pm 0.1)\times 10^{-42}\text{ cm}^2$, respectively, where hep denotes ${}^3\text{He} + p$. The cross-section uncertainty is negligible, $\pm\frac{1}{2}\%$, for the ratio of neutral-current to charged-current events. Independent of neutrino oscillations, the cross sections correspond to $4.5(1\pm 0.38)\times 10^3$ solar-neutrino events per year in the proposed one-kiloton Sudbury Neutrino Observatory if the standard solar model is correct. For a galactic supernova, the total number of neutral-current events expected in the Sudbury detector is about 10^3 (distance/8 kpc) $^{-2}$; most of the signal is expected to arise from μ and τ neutrinos and antineutrinos. If either μ or τ neutrinos have a mass greater than $2\times 10^2\text{ eV}$, then this mass should be measurable using the neutrino signal from a galactic supernova.

I. INTRODUCTION

How can we "solve" the solar-neutrino problem? The observed rate at which ${}^8\text{B}$ solar neutrinos are detected at Earth in the ${}^{37}\text{Cl}$ (Refs. 1 and 2) and the Kamiokande II (Refs. 3 and 4) (neutrino-electron scattering) experiments is less than one-half the rate calculated from the standard solar model.^{5,6} This discrepancy between calculation and observation has existed at about the same level for two decades.^{7,8} Many theoretical explanations have been suggested, some involving new weak-interaction physics and some requiring changes in our quantitative ideas of how stars evolve. An almost equally large number of possible solar-neutrino experiments have been proposed, most of which involve charged-current neutrino absorption. Each of the proposed experiments will test some aspect of at least one suggested theoretical explanation.

Recently, several authors⁹⁻¹¹ have stressed the idea that pure neutral-current reactions can provide a decisive test of whether the Sun produces neutrinos with a flux and energy spectrum that are consistent with the standard solar model. Neutral-current interactions are the same, in the standard model of weak-interaction physics, independent of the flavor (electron, muon, or τ) in which the neutrinos reach the Earth. In particular, if the attractive explanation of resonant neutrino oscillations [hereafter referred to as the Mikheyev-Smirnov-Wolfenstein (MSW) effect^{12,13}] is correct, then a neutral-current experiment will register events at the same rate as if there were no matter effects on the solar neutrino. Neutral-current experiments are *blind* to MSW effects. Recent studies by Sudbury Neutrino Observatory Colla-

boration¹⁴ have shown that the neutral-current disintegration of deuterium by ${}^8\text{B}$ solar neutrinos can be observed with the proposed one-kiloton D_2O detector.¹⁴

We have, therefore, undertaken a detailed study of the neutrino cross sections for the neutral-current disintegration of deuterium. Section II contains a derivation of the effective nuclear transition operators and a numerical evaluation of the cross sections. We have estimated the meson-exchange contribution for two different sets of coupling constants. The cross sections are calculated with and without the meson-exchange correction using two different nuclear potentials. We have estimated the range of the nuclear-physics ambiguity from the results obtained with different assumptions. Section III presents the neutrino disintegration cross sections averaged over the solar ${}^8\text{B}$ and hep (${}^3\text{He} + p$) neutrino energy spectra. The total theoretical uncertainty, defined as in Bahcall *et al.*,^{5,6} is $\pm 10\%$. Supernovae can also be studied effectively using neutral-current interactions. In Sec. IV we calculate the number of events expected in the Sudbury detector from a galactic supernova and show that most of the events are caused by μ and τ neutrinos (and antineutrinos). If either μ or τ neutrinos have masses in excess of 200 eV, then the massive neutrinos will be separated clearly in time of arrival from the less massive electron neutrinos. In order to facilitate future analyses of supernova detection with the Sudbury detector, we give in Sec. IV the neutrino and antineutrino disintegration cross sections as a function of incident neutrino energy. We compare the present results with those of the existing literature in Sec. V. The neutron energy spectrum is represented by a convenient fitting formula in Sec. VI. The summary discussion is given in Sec. VII.

II. CALCULATION OF TOTAL CROSS SECTION

We describe here the calculation of the total cross sections for the neutral-current reactions:

$$\nu + d \rightarrow \nu' + n + p, \quad (1a)$$

$$\bar{\nu} + d \rightarrow \bar{\nu}' + n + p. \quad (1b)$$

We start with the effective Hamiltonian for neutral currents:¹⁵

$$H_{\text{eff}} = \frac{G}{\sqrt{2}} J_{\mu}^{(0)} l_{\mu}, \quad (2)$$

where G ($=1.01 \times 10^5/m_p^2$) is the weak-coupling constant. The lepton current l_{μ} is written as $l_{\mu} = \bar{u}_{\nu} \gamma_{\mu} (1 + \gamma_5) u_{\nu}$ for the reaction (1a) and $l_{\mu} = \bar{v}_{\nu} \gamma_{\mu} (1 + \gamma_5) v_{\nu}$ for the reaction (1b). The hadronic neutral current $J_{\mu}^{(0)}$ in the standard [Weinberg-Salam-Glashow-Iliopoulos-Maiani (GIM)] model is given by

$$J_{\mu}^{(0)} = V_{\mu}^3 + A_{\mu}^3 - 2 \sin^2 \theta_w (V_{\mu}^S + V_{\mu}^3). \quad (3)$$

Here, V_{μ}^S is the isoscalar vector current, V_{μ}^i ($i=1,2,3$) the isovector vector current, and A_{μ}^i ($i=1,2,3$) the isovector axial-vector current; θ_w ($\sin^2 \theta_w = 0.25$) is the Weinberg angle. (Since the leading-order impulse approximation term does not depend on the Weinberg an-

gle, the precise value adopted is unimportant. For example, changing $\sin^2 \theta_w$ from 0.25 to 0.23 only changes the neutral-current disintegration cross section by 0.2% for a neutrino energy of 15 MeV.) We decompose the hadronic current $J_{\mu}^{(0)}$ into isoscalar and isovector pieces for convenience of the following discussion:

$$J_{\mu}^{(0)} = J_{\mu}^{T=0} + J_{\mu}^{T=1},$$

where

$$J_{\mu}^{T=0} = -2 \sin^2 \theta_w V_{\mu}^S$$

and

$$J_{\mu}^{T=1} = (1 - 2 \sin^2 \theta_w) V_{\mu}^3 + A_{\mu}^3.$$

In reactions (1a) and (1b), the initial deuteron has isospin $T=0$, whereas the final p - n state can have both $T=0$ and 1. On the other hand, in the cases of the charged current, i.e., $\nu_e + d \rightarrow e^{-} + p + p$ and $\bar{\nu}_e + d \rightarrow e^{+} + n + n$, the final two nucleon states (p - p and n - n) have only $T=1$. However, we can demonstrate that the neutral-current reaction is simply related to the charged-current reactions by the isospin rotation as long as higher-order terms are neglected. The discussion is as follows. The cross section σ for the reactions (1a) and (1b) is written as

$$\sigma \sim \int (\text{phase space}) \delta^{(4)}(p_{\nu} + P_f - p_{\nu'} - P_i) \sum_f \langle i | J_{\lambda}^{(0)\dagger} | f \rangle \langle f | J_{\mu}^{(0)} | i \rangle \sum_{\text{spins}} \langle \nu | l_{\lambda} | \nu' \rangle \langle \nu' | l_{\mu} | \nu \rangle, \quad (4)$$

where $|i\rangle$ and $|f\rangle$ stand for the initial and final two-nucleon states, respectively. To concentrate on the isospin structure, let us write $|i\rangle = |\xi_i; T=0,0\rangle$ and $|f\rangle = |\xi_f; T, T_z\rangle$, where ξ_i (ξ_f) are any additional quantum numbers necessary to specify $|i\rangle$ ($|f\rangle$). After a short calculation of the isospin Clebsch-Gordan coefficients, the hadron part in Eq. (4) is written as

$$\begin{aligned} & \sum_{T, T_z} \langle \xi_i; T=0,0 | J_{\lambda}^{(0)\dagger} | \xi_f; T, T_z \rangle \langle \xi_f; T, T_z | J_{\mu}^{(0)} | \xi_i; T=0,0 \rangle \\ & = \langle \xi_i; T=0,0 | J_{\lambda}^{T=0\dagger} | \xi_f; T=0,0 \rangle \langle \xi_f; T=0,0 | J_{\mu}^{T=0} | \xi_i; T=0,0 \rangle \\ & + \sum_{T_z} \langle \xi_i; T=0,0 | J_{\lambda}^{T=1\dagger} | \xi_f; T=1, T_z \rangle \langle \xi_f; T=1, T_z | J_{\mu}^{T=1} | \xi_i; T=0,0 \rangle. \quad (5) \end{aligned}$$

The treatment so far is exact, but we now introduce an approximate argument relying on the smallness of the energies involved in the solar neutrino reaction. In the low-energy regime, the lowest-order impulse approximation (IA) terms give dominant contributions, and higher-order IA terms and meson-exchange currents (MEC) constitute significant but not too large corrections to the leading-order IA terms. Thus, compared with the leading IA term ~ 1 , the corrections due to next-order IA terms and MEC are $O(\epsilon)$, $\epsilon \leq 0.1$. We do need and will calculate effects of $O(\epsilon)$ in the cross section σ in order to obtain a quantitative assessment of the reliability of the IA results, but terms of $O(\epsilon^2)$ can be ignored with no serious consequences. We examine the isoscalar piece $J_{\lambda}^{T=0}$ in this context. Let us observe that $J_{\mu}^{T=0} = V_{\mu}^S$, and that, in IA, $V_{\mu}^S = \bar{\psi}_N \gamma_{\mu} \psi_N$, and so $V_{\mu}^S (\mu=1,2,3) = O(\epsilon)$ whereas $V_{\mu=0}^S \rightarrow 1$. The identity operator coming from

the time component can never cause nuclear transition, and therefore can be dropped. Then, $\langle f | V_{\mu}^S | i \rangle = O(\epsilon)$, and consequently the first term in Eq. (5) is

$$\langle i | J_{\lambda}^{T=0\dagger} | f \rangle \langle f | J_{\mu}^{T=0} | i \rangle = O(\epsilon^2). \quad (6)$$

Therefore, in evaluating (5), we need to retain only the isovector current $J_{\lambda}^{T=1}$ and only the $T=1$ component of the final state.

The smallness of the incident neutrino energy E_{ν} ($E_{\nu} < 40$ MeV) also means that, in the final two-nucleon system of the reactions (1a) and (1b), the relative motion can be assumed to be in s wave. Thus, the final state $|f\rangle$ can be written as

$$|f\rangle = |np; T=1, T_z=0, S=0, L=0; J=0\rangle. \quad (7)$$

The initial deuteron state is expressed as

$$|i\rangle = \sum_{L=0,2} |d; T=0, T_z=0, (S=1, L); J=1, M_i\rangle, \quad (8)$$

where M_i is the spin substate of the deuteron. Let us proceed to consider the matrix element

$$\begin{aligned} \langle f | J_\mu^{T=1} | i \rangle &= (1 - 2 \sin^2 \theta_W) \langle f | V_\mu^3 | i \rangle \\ &+ \langle f | A_\mu^3 | i \rangle. \end{aligned} \quad (9)$$

Obviously, only those pieces of V_μ^3 and A_μ^3 that contain spin operators can contribute to (9). For V_μ^3 , however, the spin-dependent operator in IA appears as a recoil term, i.e., $\mathbf{V}^3 \sim \tau^3(\boldsymbol{\sigma} \times \mathbf{k})/M_N = O(\epsilon)$. Since MEC effects are corrections of $O(\epsilon)$ in reference to this IA term of $O(\epsilon)$, we need not consider the MEC for V_μ^3 for the present purpose. By contrast, $\langle f | A_\mu^3 | i \rangle$ does have a contribution ~ 1 coming from $\mathbf{A}^3 \sim \tau^3 \boldsymbol{\sigma}$, and, therefore, one must estimate the contributions of the MEC along with those of next-order IA terms.

To write down explicit expressions for the effective nuclear transition operators, let us first define the nucleon form factors:

$$\begin{aligned} \langle N(p') | V_\lambda^3(0) | N(p) \rangle \\ = \bar{u}(p') (g_V \gamma_\lambda + g_M \sigma_{\lambda\mu} k_\mu) \frac{\tau^3}{2} u(p), \end{aligned} \quad (10a)$$

$$\begin{aligned} \langle N(p') | A_\lambda^3(0) | N(p) \rangle \\ = \bar{u}(p') (g_A \gamma_\lambda + i g_P k_\lambda) \gamma_5 \frac{\tau^3}{2} u(p), \end{aligned} \quad (10b)$$

where $k = p - p'$, $g_A = 1.26$, and $g_M = 3.7/2M_N$. We have dropped form factors corresponding to second-class currents. (A summary of the nuclear-physics information on the upper limit of the second-class current can be found in Ref. 16.)

By using the standard nonrelativistic reduction, and by retaining only those terms of $O(\epsilon)$ which have appropriate selection rules for the $|f\rangle$ and $|i\rangle$ of Eqs. (7) and (8), we can derive the effective nuclear transition operator $H_{\text{eff}}^{\text{IA}}$ describing the IA contributions:

$$H_{\text{eff}}^{\text{IA}} = \frac{G}{\sqrt{2}} i \sum_{i=1,2} \frac{\tau_i^3}{2} [\mathbf{B}_i \cdot \mathbf{l}(\mathbf{r}_i) + A_i l_0(\mathbf{r}_i)], \quad (11)$$

where

$$A_i = g_A \frac{\boldsymbol{\sigma}_i \cdot \mathbf{k}}{2M_N}, \quad (12a)$$

$$\mathbf{B}_i = g_A \boldsymbol{\sigma}_i + (g'_V + 2M_N g'_M) \frac{i(\boldsymbol{\sigma}_i \times \mathbf{k})}{2M_N}, \quad (12b)$$

$$g'_V = (1 - 2 \sin^2 \theta_W) g_V, \quad (13)$$

$$g'_M = (1 - 2 \sin^2 \theta_W) g_M.$$

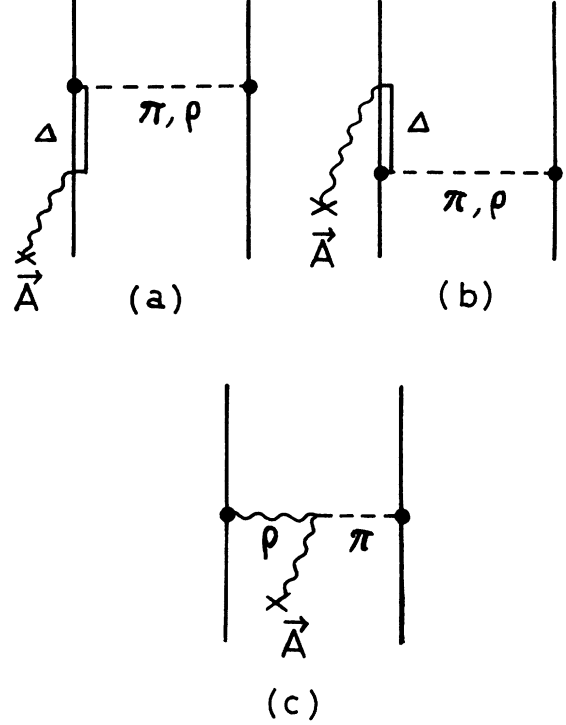


FIG. 1. Diagrams of the meson-exchange currents. (a) π exchange with Δ excitation, (b) ρ exchange with Δ excitation, and (c) $\rho\pi$ current diagrams.

As mentioned earlier, for the space component of the axial-vector current A_λ^3 , we need to include also the MEC terms. It is useful to recall at this point that there exist in the literature a great many studies dealing with the MEC for the charged current $A_\lambda^1 \pm i A_\lambda^2$. Specifically, for the $A=2$ system, a detailed calculation of the cross section for $\nu_e + d \rightarrow e^- + p + p$ was recently reported in Ref. 17 (to be referred to as NKKK).

By invoking the Wigner-Eckart theorem in isospin space, the MEC used by NKKK can be easily translated into the present neutral-current case. The result is that the effective nuclear transition Hamiltonian H_{eff} is given by

$$H_{\text{eff}} = H_{\text{eff}}^{\text{IA}} + H_{\text{eff}}^{\text{MEC}} \quad (14)$$

with

$$H_{\text{eff}}^{\text{MEC}} = \frac{G}{\sqrt{2}} i \mathbf{A}_{\text{MEC}} \cdot \mathbf{l}(\mathbf{r}), \quad (15)$$

where

$$\mathbf{A}_{\text{MEC}} = \mathbf{A}_{\text{MEC}}^\Delta + \mathbf{A}_{\text{MEC}}^{\rho\pi}$$

is the meson-exchange current operator corresponding to Fig. 1. The operators $\mathbf{A}_{\text{MEC}}^\Delta$ and $\mathbf{A}_{\text{MEC}}^{\rho\pi}$ are written as

$$\begin{aligned} \mathbf{A}_{\text{MEC}}^\Delta = \xi^\Delta \left[\left(\frac{\boldsymbol{\tau}_1 \times \boldsymbol{\tau}_2}{2} \right)^3 \left[\frac{2}{3} (\boldsymbol{\sigma}_1 \times \boldsymbol{\sigma}_2) f_0(x_\pi, x_\rho, 2c^\Delta) - \mathbf{T}_{12}^{(\times)} f_2(x_\pi, x_\rho, -c^\Delta) \right] \right. \\ \left. - 2 \left(\frac{\boldsymbol{\tau}_1 - \boldsymbol{\tau}_2}{2} \right)^3 \left[\frac{1}{3} (\boldsymbol{\sigma}_1 - \boldsymbol{\sigma}_2) f_0(x_\pi, x_\rho, 2c^\Delta) + \mathbf{T}_{12}^{(-)} f_2(x_\pi, x_\rho, -c^\Delta) \right] \right] \end{aligned} \quad (16a)$$

and

$$\mathbf{A}_{\text{MEC}}^{\rho\pi} = \xi^{\rho\pi} \left[\frac{\boldsymbol{\tau}_1 \times \boldsymbol{\tau}_2}{2} \right]^3 \left[\frac{2}{3} (\boldsymbol{\sigma}_1 \times \boldsymbol{\sigma}_2) f_0(x_\pi, x_\rho, -c^{\rho\pi}) - \mathbf{T}_{12}^{(\times)} f_2(x_\pi, x_\rho, -c^{\rho\pi}) \right], \quad (16b)$$

where ξ^Δ , $\xi^{\rho\pi}$, c^Δ , and $c^{\rho\pi}$ are the coupling constants which we discuss later on. In Eq. (16),

$$\mathbf{T}_{12}^\odot = (\boldsymbol{\sigma}_1 \odot \boldsymbol{\sigma}_2) \cdot \hat{\mathbf{r}} \mathbf{r} - \frac{1}{3} (\boldsymbol{\sigma}_1 \odot \boldsymbol{\sigma}_2) \quad (\odot = - \text{ or } \times)$$

is the spin tensor operator, and

$$f_0(x_\pi, x_\rho, \alpha) = V_0(x_\pi) + \alpha V_0(x_\rho),$$

$$f_2(x_\pi, x_\rho, \alpha) = V_2(x_\pi) + \alpha V_2(x_\rho)$$

$$(\alpha = 2c^\Delta, -c^\Delta, \text{ and } -c^{\rho\pi}),$$

where

$$V_0(x_i) = Y_0(x_i) - (\Lambda_i/m_i)^3 Y_0(x_{\Lambda_i}) \\ + [\Lambda_i(\Lambda_i^2 - m_i^2)/2m_i^3](2 - x_{\Lambda_i}) Y_0(x_{\Lambda_i})$$

$$\xi^\Delta = 0.133g_A/4 = 4.19 \times 10^{-2},$$

$$\xi^{\rho\pi} = (f_{\pi NN}^2/4\pi)(m_\rho/m_\pi)[(g_V + 2M_N g_M)/g_A] m_\rho^2/(m_\rho^2 - m_\pi^2) = 5.63 \times 10^{-2},$$

$$c^\Delta = 0.834(m_\rho/m_\pi)^3, \text{ and } c^{\rho\pi} = (m_\rho/m_\pi)^3.$$

On the other hand, model B gives

$$\xi^\Delta = \frac{16}{25}(g_A f_{\pi NN}^2/4\pi)m_\pi/(M_\Delta - M_N) = 3.14 \times 10^{-2},$$

$$\xi^{\rho\pi} = f_{\pi NN} f_{\rho NN} [(1 + K_V)/4\pi] \sqrt{2} m_\pi^2/(m_\rho^2 - m_\pi^2) = 3.15 \times 10^{-2},$$

$$c^\Delta = [f_{\rho NN}^2(1 + K_V)^2/4\pi]/(f_{\pi NN}^2/4\pi) = 3.62 \times 10^2, \text{ and } c^{\rho\pi} = (m_\rho/m_\pi)^3.$$

(The expression [Eq. (16)] of $\mathbf{A}_{\text{MEC}} = \mathbf{A}_{\text{MEC}}^\Delta + \mathbf{A}_{\text{MEC}}^{\rho\pi}$ is completely equivalent to the expression [Eq. (15)] given by NKKK except for the isospin operators.)

We have now a full expression for H_{eff} to be sandwiched between $|f\rangle$ and $|i\rangle$ of Eqs. (7) and (8). By squaring the resulting transition matrix element, and integrating over the final momenta, the total cross section σ for the reactions (1a) and (1b) is obtained as

$$\sigma = \frac{G^2 g_A^2}{4\pi^3} \int dE_\nu E_\nu'^2 (M_N^3)^{1/2} \sqrt{E_{\text{rel}}} J_0^2 \Lambda, \quad (17)$$

where E_ν and E_ν' are initial and final neutrino energies (or initial and final antineutrino energies), respectively, and $E_{\text{rel}} = E_\nu - E_\nu' - |\epsilon|$ is the relative motion energy of the outgoing neutron and proton. (Here $\epsilon = -2.225$ MeV is the binding energy of the deuteron.) Furthermore,

$$\Lambda = 1 + 2\delta^{\text{MEC}} \pm \frac{1}{3} \gamma'(E_\nu + E_\nu')/M_N - \frac{1}{3}(E_\nu - E_\nu')/M_N, \quad (18)$$

where upper and lower signs correspond to the reactions (1a) and (1b), respectively. In Eq. (18), $\gamma' = (g_V' + 2M_N g_M')/g_A$ and

and

$$V_2(x_i) = Y_2(x_i) - (\Lambda_i/m_i)^3 Y_2(x_{\Lambda_i}) \\ + [\Lambda_i(\Lambda_i^2 - m_i^2)/2m_i^3](1 + x_{\Lambda_i}) Y_0(x_{\Lambda_i}).$$

Here $x_i = m_i r$, $i = \pi$ and ρ , and $Y_0(x) = e^{-x}/x$ and $Y_2(x) = (e^{-x}/x)(1 + 3/x + 3/x^2)$. The values $\Lambda_\pi = 1.0$ GeV and $\Lambda_\rho = 1.44$ GeV are used for the cutoff parameters of the meson-baryon vertices.¹⁸ The constants ξ^Δ , $\xi^{\rho\pi}$, c^Δ , and $c^{\rho\pi}$ in Eq. (16) involve the combination of coupling constants for various vertices in Fig. 1, and have some model dependence. We use here what NKKK call model A (Ref. 19) and model B (Ref. 20). Model A gives

$$\delta^{\text{MEC}} = \xi^{\rho\pi}/g_A \left[\frac{4}{3} Y_0/J_0 + \frac{2\sqrt{2}}{3} (Y_2 - \xi^\Delta/\xi^{\rho\pi} Y_2')/J_0 \right], \quad (19)$$

with

$$J_0 = \langle \varphi_{np}(r); L=0 | j_0(kr/2) | \varphi_d(r); L=0 \rangle, \quad (20a)$$

$$Y_0 = \langle \varphi_{np}(r), L=0 | f_0(x_\pi, x_\rho, -c^{\rho\pi}) | \varphi_d(r), L=0 \rangle, \quad (20b)$$

$$Y_2 = \langle \varphi_{np}(r), L=0 | f_2(x_\pi, x_\rho, -c^{\rho\pi}) | \varphi_d(r), L=2 \rangle, \quad (20c)$$

$$Y_2' = \langle \varphi_{np}(r), L=0 | f_2(x_\pi, x_\rho, -c^\Delta) | \varphi_d(r), L=2 \rangle. \quad (20d)$$

In evaluating the matrix elements Eq. (20), the relative wave functions $\varphi_d(r)$ and $\varphi_{pn}(r)$ for the deuteron and the outgoing p - n state, respectively, should be obtained by solving the Schrödinger equation with realistic nucleon-nucleon potentials. Here, we use the Reid soft-core and the Reid hard-core potentials.²¹ Because of the assump-

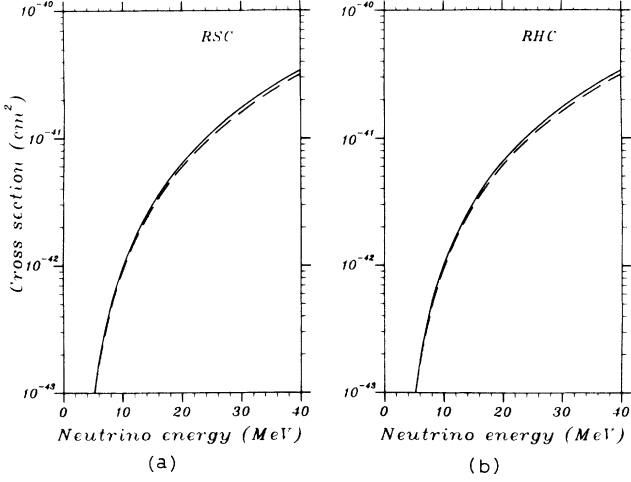


FIG. 2. Total cross sections for $\nu + d \rightarrow \nu' + n + p$ as a function of neutrino energy. (a) Reid soft-core nuclear potential. (b) Reid hard-core nuclear potential. The solid line represents the full calculation by model A and the dashed line is the impulse approximation. (The full calculation by model B is almost degenerate with the impulse approximation.)

tion of the charge independence of the strong interaction, the Reid potential gives the same values of the scattering length and the effective range for both the n - n interaction and the spin-singlet p - n interaction; for example, $a = -17.1$ fm and $r_{\text{eff}} = 2.8$ fm in the case of the soft-core potential. (In the case of the p - p interaction, they are $a = -7.78$ fm and $r_{\text{eff}} = 2.72$ fm because of the additional Coulomb potential.) The experimental values clearly show the violation of the charge independence; i.e., $a = -17.29$ fm and $r_{\text{eff}} = 2.8$ fm for the n - n interaction, whereas, $a = -23.7$ fm and $r_{\text{eff}} = 2.7$ fm for the spin-singlet p - n interaction. In order to take into account this charge dependence in the Reid potential, we modified the potential depth of the non-one-pion-exchange potential (OPEP) part by 2% in the p - n case, which reproduces the experimental p - n data satisfactorily.²¹

The calculated cross sections are given in Fig. 2 for the reaction (1a) and in Fig. 3 for the reaction (1b) as a function of E_ν . In Figs. 2 and 3, RSC (RHC) corresponds to the Reid soft- (hard-)core potential. The solid line represents the full calculation including the meson-exchange current of model A and the dashed line corresponds to model B. The dashed-dotted line is the result of the impulse approximation.

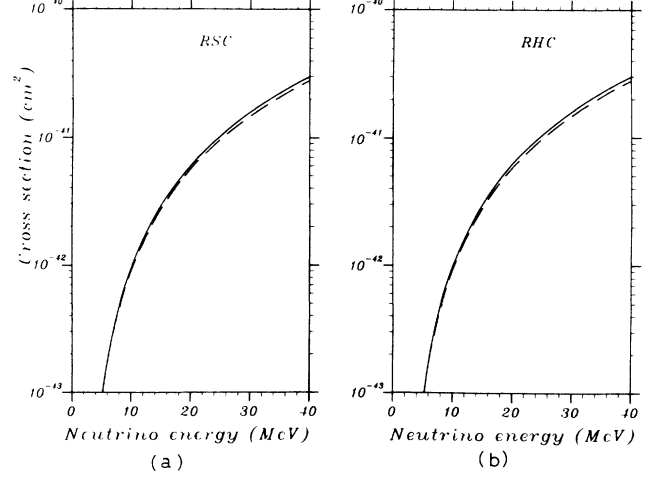


FIG. 3. Total cross sections for $\bar{\nu} + d \rightarrow \bar{\nu}' + n + p$ as a function of antineutrino energy. (a) Reid soft-core nuclear potential. (b) Reid hard-core nuclear potential. Definitions are the same as for Fig. 2.

In order to show the relative importance of the MEC and higher-order IA terms, we give the ratios of the cross sections in Tables I and II. In Tables I and II, GT denotes the leading-order IA (Gamow-Teller) contribution in the impulse approximation. We see that the contributions from the MEC and the higher-order IA terms become more important as the incident neutrino energy increases. We note that for both nuclear potentials the meson-exchange correction to the impulse approximation is typically $\sim 7\%$ and $\sim 1\%$ in model A and model B, respectively. We consider this difference as representative of the uncertainty in the determination of the vertices that give rise to the exchange currents. Thus, as far as the final s -wave contribution is concerned, it is conservative to use 10% error bars for the cross sections obtained by state-of-the-art calculations, such as the present evaluation.

So far we have neglected higher partial waves than s wave in the n - p final state. One of the typical matrix elements appearing in the next-order p -wave contribution is

$$J_1^J = \langle \varphi_{np}^J(r); L=1 | j_1(kr/2) | \varphi_d(r); L=0 \rangle,$$

where J ($=0, 1, 2$) is the total angular momentum quantum number. [The leading-order s -wave matrix element J_0 is given by Eq. (20a).] Therefore, we expect that the ratio of the p -wave contribution to the s -wave contribu-

TABLE I. Ratios of the total cross sections of $\nu + d \rightarrow \nu' + n + p$. Here RSC (RHC) denotes the Reid soft- (hard-)core nuclear potential.

Nuclear potential	Neutrino energy (MeV)	$\sigma^{\text{IA}}/\sigma^{\text{GT}}$	$\sigma^{\text{IA+MEC}}/\sigma^{\text{GT}}$	
			Model A	Model B
RSC	20	1.03	1.10	1.04
	40	1.06	1.14	1.07
RHC	20	1.03	1.10	1.04
	40	1.06	1.14	1.08

TABLE II. Ratios of the total cross sections of $\bar{\nu} + d \rightarrow \bar{\nu}' + n + p$. Definitions are the same as in Table I.

Nuclear potential	Neutrino energy (MeV)	σ^{IA}/σ^{GT}	$\sigma^{IA+MEC}/\sigma^{GT}$	
			Model A	Model B
RSC	20	0.970	1.04	0.980
	40	0.940	1.01	0.950
RHC	20	0.970	1.04	0.980
	40	0.940	1.01	0.950

tion is roughly given by $J_1^J/J_0 \simeq [j_1(kR)]^2$, where $R = 4$ fm is the root-mean-square radius of the deuteron. This ratio is $\lesssim 3\%$ for solar neutrinos ($E_\nu \leq 20$ MeV), and therefore well within the theoretical uncertainty $\sim 10\%$ assigned to the s -wave contribution. We therefore consider that the total uncertainty in the cross sections calculated in this work is $\lesssim 10\%$ for the energy regime of solar neutrinos. For supernova neutrinos with energies $E_\nu \leq 40$ MeV, the ratio of p wave to s wave amounts to $\sim 15\%$. This uncertainty may be combined with the uncertainty in the s -wave contribution to give an identifiable total uncertainty $\lesssim 20\%$. However, taking into account the discussion in Sec. V, where we compare the present calculation with previous studies, it seems prudent to assign somewhat larger uncertainties to the theoretical cross sections. We argue in Sec. V that, for neutrinos with energies $E_\nu \leq 40$ MeV, it is reasonable to assign error bars of 40% to the cross sections calculated here.

III. SOLAR NEUTRINOS

The two most important sources of solar neutrinos for the neutral-current disintegration of deuterium are ^8B and hep neutrinos (see Ref. 6). None of the other sources emit neutrinos that are above the 2.225-MeV threshold for the disintegration of deuterium.

We show in Table III the disintegration cross sections for reaction (1a) that are averaged over the known spectrum of ^8B neutrinos²² and hep neutrinos.⁶ The meaning of the symbols is the same as in Table I. We conclude from Table III that the average cross sections for solar neutrinos are well determined. The results may be summarized as follows:

$$\langle \sigma(^8\text{B}) \rangle = 0.41(1 \pm 0.1) \times 10^{-42} \text{ cm}^2 \quad (21)$$

and

$$\langle \sigma(\text{hep}) \rangle = 1.15(1 \pm 0.1) \times 10^{-42} \text{ cm}^2. \quad (22)$$

The uncertainties that are in Eqs. (21) and (22) are “total theoretical uncertainties” as defined in Ref. 6.

Using the fluxes of neutrinos calculated from the standard solar model,⁶ we can now estimate the rate at which neutral-current-induced disintegrations of deuterium are expected to occur in the one-kiloton D_2O Sudbury Neutrino Observatory. (The number of deuterium nuclei in the detector is 6.02×10^{31} .) We find that the expected number of events is (assuming 100% detection efficiency)

$$\text{neutral-current events} = 4.5(1 \pm 0.38) \times 10^3 \text{ yr}^{-1} \text{ kton}^{-1}. \quad (23)$$

Almost all of the events are expected to arise from ^8B neutrinos; less than 1% of the total rate is due to hep neutrinos if the standard solar model is correct. The uncertainty shown in the predicted event rate [Eq. (23)] is dominated by the 37% uncertainty in the calculated ^8B neutrino flux.

IV. SUPERNOVA NEUTRINOS

A neutral-current measurement of the total neutrino flux from a galactic supernova would be an important diagnostic test of our understanding of supernova processes and would also provide a marvelous laboratory for doing weak-interaction physics.¹⁴ We have, therefore, tabulated in Table IV the disintegration cross sections for reaction (1a) as a function of the incident neutrino energies. The mean values of model A and model B are listed. As discussed at the end of the preceding section, our calculations are estimated to be accurate to better than 40% even at the highest energy considered here, $E_\nu = 40$ MeV. This accuracy is sufficient for most astrophysical purposes since the uncertainties in the calculated neutrino fluxes from supernovae is at least of order a factor of 2 or 3.

Antineutrinos are expected to be produced almost as

TABLE III. Neutral-current cross sections for solar neutrinos.

Nuclear potential	Effective operator	$\langle \sigma(^8\text{B}) \rangle$ ($\times 10^{-42} \text{ cm}^2$)	$\langle \sigma(\text{hep}) \rangle$ ($\times 10^{-42} \text{ cm}^2$)
RSC	IA	0.40	1.11
	IA + MEC (model A)	0.43	1.20
	IA + MEC (model B)	0.40	1.13
RHC	IA	0.40	1.11
	IA + MEC (model A)	0.43	1.20
	IA + MEC (model B)	0.40	1.13

TABLE IV. Neutral-current cross sections for individual neutrino energies. The mean values of models A and B are listed

Neutrino energy (MeV)	$\sigma^{\text{IA+MEC}}$ ($\times 10^{-42}$ cm ²)	Neutrino energy (MeV)	$\sigma^{\text{IA+MEC}}$ ($\times 10^{-42}$ cm ²)
2.5	1.1×10^{-4}	10.5	1.1
3.0	2.5×10^{-3}	11.0	1.3
3.5	1.1×10^{-2}	11.5	1.5
4.0	2.5×10^{-2}	12.0	1.6
4.5	5.0×10^{-2}	12.5	1.9
5.0	8.0×10^{-2}	13.0	2.0
5.5	1.3×10^{-1}	14.0	2.5
6.0	1.7×10^{-1}	15.0	3.0
6.5	2.4×10^{-1}	16.0	3.5
7.0	3.0×10^{-1}	17.0	4.2
7.5	4.0×10^{-1}	18.0	4.8
8.0	4.9×10^{-1}	20.0	6.3
8.5	5.8×10^{-1}	25.0	11
9.0	6.9×10^{-1}	30.0	17
9.5	8.4×10^{-1}	35.0	24
10.0	9.7×10^{-1}	40.0	33

copiously as neutrinos in explosions of (matter) supernova. We have calculated, therefore, the ratio R of neutrino-induced to antineutrino-induced deuterium disintegrations. Explicitly,

$$R = \frac{\sigma(\nu + d \rightarrow \nu' + n + p)}{\sigma(\bar{\nu} + d \rightarrow \bar{\nu}' + n + p)}. \quad (24)$$

Note that R is exactly equal to unity in the usual approximation of allowed β decay and only differs from unity by terms of order (v_{nucleon}/c) . (See discussion in Sec. II.)

Table V contains numerical values for R that were obtained using different nuclear potentials. We estimate that the values of R given in Table V are accurate to about 1% or better. For some estimates, the approximation $R = [0.994 + 0.0034(E_\nu/\text{MeV})]$, may be useful, where E_ν is the incident neutrino energy.

The neutrinos produced by supernova explosions can be described approximately by a Maxwell-Boltzmann spectrum, according to the works of several authors.²³⁻²⁹

TABLE V. The ratio R of neutrino-induced to antineutrino-induced disintegration of the deuteron. The quantity R is defined in Eq. (24).

Neutrino energy (MeV)	Ratio R	Neutrino energy (MeV)	Ratio R
3.0	1.006	12.0	1.034
4.0	1.009	14.0	1.041
5.0	1.011	16.0	1.047
6.0	1.015	18.0	1.054
7.0	1.018	20.0	1.061
8.0	1.020	25.0	1.078
9.0	1.024	30.0	1.095
10.0	1.028	35.0	1.114
11.0	1.031	40.0	1.130

TABLE VI. Thermally averaged neutral-current cross sections.

Neutrino temperature (MeV)	$\sigma(\nu)$ ($\times 10^{-42}$ cm ²)	$\sigma(\bar{\nu})$ ($\times 10^{-42}$ cm ²)
2	0.41	0.39
3	1.3	1.25
4	2.6	2.5
5	4.4	4.1

We present, therefore, in Table VI the cross sections for neutrinos with thermal temperatures between 2 and 5 MeV; the best estimate for the average temperature for electron-type antineutrinos from the Large Magellanic Cloud (LMC) supernova is about 4.1 MeV (Refs. 28 and 29).

The total fluence of neutrinos (ν_e , ν_μ , and ν_τ), as distinct from antineutrinos ($\bar{\nu}_e$) was not well determined²⁹ by the normal water (proton) detectors, Kamiokande II³⁰ and Irvine-Michigan-Brookhaven³¹ (IMB). However, preobservation expectations²⁹ are consistent with the observed^{30,31} fluence of $\bar{\nu}_e$ detection rates to within a factor of 2 (Ref. 29). This consistency suggests that the fluence of neutrinos may also be reasonably well predicted by the model calculations, again to an accuracy of order a factor of 2 or 3. For a type-II supernova in the Galaxy, one therefore estimates fluences^{23,29}

$$\phi(\nu_e) = 2.4 \times 10^{11} \text{ cm}^{-2} \left[\frac{8 \text{ kpc}}{\text{distance}} \right]^2 \quad (25a)$$

and $\phi(\nu_\mu) = \phi(\bar{\nu}_\mu) = \phi(\nu_\tau) = \phi(\bar{\nu}_\tau)$, with

$$\phi(\bar{\nu}_\mu) = 1.7 \times 10^{11} \text{ cm}^{-2} \left[\frac{8 \text{ kpc}}{\text{distance}} \right]^2 \quad (25b)$$

and $\phi(\bar{\nu}_e) \sim 0.7\phi(\nu_e)$. Plausible values of the neutrino temperatures are^{23,29}

$$T(\nu_e) \approx T(\bar{\nu}_e) \approx 4 \text{ MeV}, \quad (25c)$$

and, with an uncertainty of at least 25%,

$$T(\nu_\mu) = T(\bar{\nu}_\mu) = T(\nu_\tau) = T(\bar{\nu}_\tau) = 10 \text{ MeV}. \quad (25d)$$

For these parameters, the total number of events in a kiloton detector of D₂O, like the Sudbury Neutrino Observatory, is

$$\text{total events} \sim 10^3 \left[\frac{8 \text{ kpc}}{\text{distance}} \right]^2. \quad (26)$$

The event rate scales approximately as $T^{2.5}$. The total rate given in Eq. (26) is uncertain by about an order of magnitude because we do not know the absolute fluences from a supernova explosion to better than a factor of few and because we do not know accurately the temperatures and interaction cross sections of the higher-energy neutrinos that are not of the electron type. With the parameters given above, about 90% of the total event rate is from muon and τ neutrinos and antineutrinos.

Can one use a neutral-current signal to measure the mass of a (presumed) finite-mass τ or μ neutrino? Yes,

provided the mass is ≥ 200 eV. The extra travel time due to a finite-neutrino mass is

$$\Delta t = 41 \text{ sec} \left[\frac{\text{distance}}{8 \text{ kpc}} \right] \left[\frac{m_\nu}{100 \text{ eV}} \right]^2 \left[\frac{10 \text{ MeV}}{E_\nu} \right]^2. \quad (27)$$

The arrival of the electron neutrinos will be signaled by the charged-current reaction as well as the initial detection of ν_e 's and $\bar{\nu}_e$'s from the neutral current. We have integrated the charged-current cross sections given by NKKK and Ref. 6 over a Maxwell-Boltzmann distribution making an approximate correction for the contribution from energies above 20 MeV. We estimate a cross section of $6 \times 10^{-42} \text{ cm}^2$ for a temperature of 4 MeV. Thus, the number of charged-current interactions from a galactic supernova is expected to be of order

$$\text{total charged current events} \sim 10^2 \left[\frac{8 \text{ kpc}}{\text{distance}} \right]^2. \quad (28)$$

The charged current should provide a clear and experimentally distinct signal which establishes when the electron neutrinos arrive.

For SN1987A, electron-type neutrinos arrived over a period of less than 15 sec. Thus neutrinos of the μ or τ flavor should arrive at a distinctly later time provided either neutrino has a mass of 200 eV. Since a kiloton detector should experience $\geq 10^2$ events each from μ and τ neutrinos, there should be enough signal to make a good mass measurement or to set a useful upper limit.³²

V. COMPARISON WITH PREVIOUS CALCULATIONS

Many theoretical studies have evaluated the neutral-current disintegration of deuterium.³³⁻³⁸ We describe here the comparison of the present results with existing literature. In order to check our results for solar and supernova neutrinos, we have repeated a number of the previous reactor and muon decay calculations. Our results are in generally good agreement with these earlier studies, although in a number of cases we have made improvements in the calculations which cause our numbers to differ significantly from some published results.

For reactor antineutrinos, we recalculated the average cross sections $\langle \sigma_{\text{reactor}} \rangle$ for reaction (1b) using the same antineutrino fluxes as used in Refs. 34 and 37. In these references, three sets of antineutrino fluxes are used, which are called No. 1, No. 2, and No. 3, respectively. We obtained $\langle \sigma_{\text{reactor}} \rangle = 6.3$ (No. 1), 4.7 (No. 2), and 4.0 (No. 3) in units of 10^{-45} cm^2 . The corresponding literature values are $\langle \sigma_{\text{reactor}} \rangle = 7.1, 5.1,$ and 4.4 for Ref. 34 and $\langle \sigma_{\text{reactor}} \rangle = 6.8, 5.0,$ and 4.4 for Ref. 37. In Refs. 34-36 cross sections were calculated in the impulse approximation IA using the simple effective range theory, whereas the present calculation and Refs. 37 and 38 use realistic nuclear potentials and also include meson-exchange corrections. The simple effective range theory overestimates the cross section by $\sim 10\%$. As was discussed in detail in Ref. 39, this discrepancy can be attributed to the fact that the effect of the two-nucleon short-range correlation is not included in the simplified wave functions.³⁹ In order to obtain accurate theoretical cross sections, it is very important to include final-state interac-

tions between two nucleons. There is a difference of about 8% between the results of the present calculations and those given in Ref. 37. Because some detailed information on the calculations of Ref. 37 is not available in published form, for example, the strength of coupling constants of vertices is not given, we cannot determine for sure what is the origin of the differences between our values and those of Ref. 37. But this discrepancy is within the present uncertainties of the nuclear model that are estimated in Sec. II.

In Ref. 38 the exchange currents were derived with the use of the hard-pion model Lagrangian. The main conclusion of Ref. 38 is that the exchange current enhances the impulse approximation values of the cross sections for reactions (1a) and (1b) by about 8%. This result is consistent with what we have found in the present calculation.

None of the above-mentioned earlier works evaluated the $1/M$ correction to the leading-order impulse approximation term, a correction which in principle should be taken into account commensurately with the exchange current corrections. We have made here explicit calculations of this correction. Also, the effects of the form factors at the vertices appearing in the exchange current diagrams have not previously been taken into account. In this work, we have included these form-factor effects in order to make our calculation at least as elaborate as the state-of-the-art calculation⁴⁰ done for the charged-current reactions. These improvements have not changed the previous results drastically, but we think it was important to check by explicit calculation to what extent the theoretical cross sections are stable against these improvements in the models.

Mintz³³ made use of the elementary-particle approach (EPA) to derive the transition matrix for the neutral-current process (1a) from that for the charged-current counterpart. It is noteworthy that the formalism used by Mintz to parametrize the nuclear transition form factors allows the inclusion of any partial waves in the relative motion of the final two-nucleon system. On the other hand, the usefulness of EPA diminishes if there is an appreciable breakdown of charge symmetry in the nucleon-nucleon interactions. In the present microscopic approach, by contrast, we have a definite framework (albeit model dependent) which enables us to take account of the charge symmetry breaking. It should also be noted that, since experimental data for $\nu_e + d \rightarrow e^- + p + p$ are at present available only for limited kinematical regions, the actual application of EPA requires a mapping of the nuclear form factors from one region of the momentum transfer to another. This mapping brings some model dependence and uncertainty into EPA, which in principle can be model independent (apart from the symmetry breaking).

With these general remarks in mind, we show in Table VII the cross sections for reaction (1a) obtained in EPA for the intermediate energy region $20 < E_\nu < 50$ MeV, together with those given by the present calculation. The disagreement between the two results is appreciable. The percentage difference becomes larger in the lower neutrino energy region, where the uncertainty of the present

TABLE VII. Comparison of the total cross section for $\nu + d \rightarrow \nu' + n + p$.

Neutrino energy (MeV)	σ^{36} ($\times 10^{-42}$ cm 2)	σ^{33} ($\times 10^{-42}$ cm 2)	$\sigma^{\text{present work}}$ ($\times 10^{-42}$ cm 2)
20	6.3	11	6.3
30	18	26	17
40	37	44	33
50	61	67	55

calculation is expected to decrease. On the other hand, as mentioned earlier, the omission of the p -wave contribution (and those of higher partial waves) in the present calculation becomes progressively more serious for the higher-energy regime, and therefore, we were prepared to encounter a rather significant difference between the two approaches. The difference seen in Table VII, however, seems somewhat larger than expected. In order to give some hint on whether this is chiefly because of the neglect of the p -wave contribution in our treatment, we also give in Table VII the results of Ref. 36, in which the p -wave contribution was included within the framework of the impulse approximation. The cross sections obtained in Ref. 36 fall between those of Ref. 33 and the present results, indicating that the difference between the latter two probably is not simply due to the p -wave contribution.

To summarize the above discussion, we believe that EPA as used in Ref. 33 is not significantly more model independent than our microscopic calculations. On the other hand, because of its semiempirical nature, EPA provides a useful, independent method for evaluating the cross sections for reactions (1a) and (1b). We take advantage of this comparison and consider the difference between the present results and those of EPA (Ref. 33) for $E_\nu \sim 40$ MeV as a measure of uncertainties for the cross sections for supernova neutrinos with $E_\nu < 40$ MeV. From the above argument, we assign 40% error bars to the theoretical cross sections for the largest energies considered here.

Finally we have considered reaction (1a) for the well-known neutrino spectrum from muon decay. We obtain $\langle \sigma \rangle = 2.2 \times 10^{-41}$ cm 2 , whereas Ref. 33 gives $\langle \sigma \rangle = 3.05 \times 10^{-41}$ cm 2 . These two values agree with each other within the error bars estimated here.

VI. NEUTRON SPECTRUM

In order to determine by Monte Carlo techniques the efficiency for detection of neutrinos by neutral-current disintegration, it is convenient to have a simple expression for the spectrum of neutrons that are produced. The differential cross section for the production of neutrons of energy, E_n , averaged over the incident neutrino spectrum is,

$$\frac{d\sigma}{dE_n} \simeq \text{const} \times (E_n)^{1/2} (\langle q_\nu \rangle - B - 2E_n)^2 J_0^2, \quad (29)$$

where J_0 is the overlap of the nuclear wave functions and B is the deuteron binding energy. The numerical neutron energy spectrum we have calculated is satisfactorily approximated if one uses for J_0 the analytic expression [(Eq. (B2) in Appendix B] in Lee's 1978 paper³⁴ and takes for ${}^8\text{B}$ neutrinos $\langle q_\nu \rangle \sim 7$ MeV (9 MeV for hep neutrinos).

VII. SUMMARY

We have calculated the cross sections for neutral-current disintegration of deuterium by solar and supernova neutrinos and, by using a wide variety of nuclear models, the theoretical uncertainties in the cross sections. The results can be used to help determine important characteristics of neutrinos, including their mass differences and mixing angles (from the MSW effect on solar neutrinos) and perhaps even values for the masses of μ or τ neutrinos (from supernova time-of-flight measurements).

We note that the ratio of neutral-current cross sections [see Eq. (1)] to charged-current cross sections,

$$\nu + d \rightarrow e^- + p + p, \quad (30)$$

is much less model dependent than the individual cross sections. This result is illustrated in Table VIII, which gives for different energies, the ratio r

$$r \equiv \frac{\sigma(\text{neutral current})}{\sigma(\text{charged current})} \quad (31)$$

for different assumed nuclear potentials. The maximum spread in r among the models we have considered is only $\pm \frac{1}{2}\%$. We therefore recommend that special emphasis be placed on the theoretical interpretation of the (to-be) observed ratio of the number of neutral-current to charged-current events.

TABLE VIII. The ratio r of the cross section for neutral-current events [Eq. (1a)] to the cross section for charged-current events [Eq. (29)]. Here A and B represent model A and model B, respectively.

Neutrino energy (MeV)	RSC			RHC		
	IA	IA + MEC(A)	IA + MEC(B)	IA	IA + MEC(A)	IA + MEC(B)
5	0.251	0.252	0.251	0.255	0.256	0.255
10	0.399	0.400	0.399	0.402	0.404	0.402
20	0.443	0.444	0.442	0.445	0.446	0.445
30	0.450	0.451	0.450	0.451	0.452	0.451
40	0.450	0.451	0.450	0.451	0.452	0.451

ACKNOWLEDGMENTS

We are grateful to S. Weinberg for a conversation that stimulated our interest in neutral-current reactions and to the members of the Sudbury Neutrino Observatory Collaboration for their interest in this work and for making it relevant. We especially appreciate comments and corrections by F. Boehm, C. Kim, A. B. McDonald, and D. Spergel (who pointed out an error in an early draft). One

of the authors (K.K.) wishes to express his sincere thanks to Professor G. E. Brown and the members of the Nuclear Theory Group for their kind hospitality during his sabbatical stay at Stony Brook. This research was supported in part by U.S. National Science Foundation Grant No. PHY82-17352 with the Institute for Advanced Study, and by Department of Energy Contract No. DE-AC02-76ER13001 with the State University of New York.

- *Permanent address: Department of Physics, Sophia University, Tokyo 102, Japan.
- ¹R. Davis, Jr., *Proceedings of the Seventh Workshop on Grand Unification*, ICOBAN '86, Toyama, Japan (World Scientific, Singapore, 1986), p. 237.
- ²J. K. Rowley, B. T. Cleveland, and R. Davis, Jr., in *Solar Neutrinos and Neutrino Astronomy*, edited by M. L. Cherry, W. A. Fowler, and K. Lande (AIP Conf. Proc. No. 126) (AIP, New York, 1985), p. 265.
- ³Y. Totsuka *et al.*, ICEPP Report No. UT-87-02, 1987 (unpublished).
- ⁴K. Hirata *et al.*, in *The Standard Model: Supernova 1987A*, proceedings of the Leptonic Session of the 22nd Rencontre de Moriond, Les Arcs, France, 1987, edited by J. Tran Thanh Van (Editions Frontières, Gif-sur-Yvette, 1987), p. 689.
- ⁵J. N. Bahcall, W. F. Huebner, W. H. Lubow, P. D. Parker, and R. K. Ulrich, *Rev. Mod. Phys.* **54**, 767 (1982).
- ⁶J. N. Bahcall and R. K. Ulrich, *Rev. Mod. Phys.* **60**, 297 (1988).
- ⁷J. N. Bahcall and R. Davis, *Science* **191**, 264 (1976).
- ⁸J. N. Bahcall and R. Davis, in *Essays in Nuclear Astrophysics*, edited by C. A. Barnes, D. D. Clayton, and S. Schramm, (Cambridge University Press, Cambridge, England, 1982), p. 243.
- ⁹H. H. Chen, *Phys. Rev. Lett.* **55**, 1534 (1985); G. Aardsma *et al.*, *Phys. Lett. B* **194**, 321 (1987).
- ¹⁰R. S. Raghavan, S. S. Pakvasa, and B. A. Brown, *Phys. Rev. Lett.* **57**, 1801 (1986).
- ¹¹S. Weinberg, *Int. J. Mod. Phys. A* **2**, 301 (1987).
- ¹²S. P. Mikheyev and A. Yu. Smirnov, *Nuovo Cimento* **9C**, 17 (1986).
- ¹³L. Wolfenstein, *Phys. Rev. D* **17**, 2369 (1978).
- ¹⁴Sudbury Scientific Collaboration, Sudbury Neutrino Observatory proposal, 1987 (unpublished).
- ¹⁵See, e.g., T. W. Donnelly *et al.*, *Phys. Lett.* **49B**, 8 (1974).
- ¹⁶M. Oka and K. Kubodera, *Phys. Lett.* **90B**, 45 (1980); L. Grenacs, *Annu. Rev. Nucl. Part. Sci.* **35**, 455 (1985).
- ¹⁷S. Nozawa, Y. Kohyama, T. Kaneta, and K. Kubodera, *J. Phys. Soc. Jpn.* **55**, 2636 (1986).
- ¹⁸K. Holinde, *Phys. Rep.* **68**, 121 (1981).
- ¹⁹P. Guichon and C. Samour, *Nucl. Phys.* **A382**, 461 (1982).
- ²⁰C. Bargholtz, *Phys. Lett.* **81B**, 286 (1979).
- ²¹R. V. Reid, *Ann. Phys. (N.Y.)* **50**, 411 (1968).
- ²²J. N. Bahcall and B. R. Holstein, *Phys. Rev. C* **33**, 2121 (1986).
- ²³J. R. Wilson, in *Numerical Astrophysics*, edited by J. Centrella *et al.* (Jones & Bartlett, Boston, 1986), p. 422.
- ²⁴J. T. Wilson *et al.*, *Ann. N.Y. Acad. Sci.* **470**, 267 (1986).
- ²⁵H. A. Bethe *et al.*, *Nucl. Phys.* **A234**, 487 (1979).
- ²⁶A. Burrows and J. M. Lattimer, *Astrophys. J.* **295**, 14 (1985).
- ²⁷J. R. Wilson, R. Mayle, S. E. Woosley, and T. E. Weaver, *Ann. N.Y. Acad. Sci.* **470**, 267 (1986).
- ²⁸J. N. Bahcall, A. Dar, and T. Piran, *Nature (London)* **326**, 135 (1987).
- ²⁹J. N. Bahcall, T. Piran, W. H. Press, and D. N. Spergel, *Nature (London)* **327**, b82 (1987).
- ³⁰Kamiokande II Collaboration, K. Hirata *et al.*, *Phys. Rev. Lett.* **58**, 1490 (1987).
- ³¹IMB Collaboration, R. M. Bionta *et al.*, *Phys. Rev. Lett.* **58**, 1494 (1987).
- ³²J. N. Bahcall and T. Piran, *Astrophys. J. Lett.* **267**, 77 (1983).
- ³³S. Mintz, *Phys. Rev. D* **22**, 2918 (1980).
- ³⁴H. C. Lee, *Phys. Lett.* **87B**, 18 (1979); *Nucl. Phys.* **A294**, 473 (1978).
- ³⁵T. Ahrens and T. P. Lang, *Phys. Rev. C* **3**, 979 (1971); T. Ahrens and L. Gallaher, *Phys. Rev. D* **20**, 2714 (1979).
- ³⁶A. Ali and C. A. Dominguez, *Phys. Rev. D* **12**, 3673 (1975).
- ³⁷W. Müller and M. Gari, *Phys. Lett.* **102B**, 389 (1981); F. T. Avignone, *Phys. Rev. D* **24**, 778 (1981).
- ³⁸J. Hosek and E. Truhlik, *Phys. Rev. C* **23**, 665 (1981).
- ³⁹F. Dautry, M. Rho, and D. O. Riska, *Nucl. Phys.* **A264**, 507 (1976).
- ⁴⁰Chr. Bargholtz, *Astrophys. J.* **233**, L161 (1979).